$\{Mn^{II}_9W^{V}_6\}_n$ Nanowires Organized into 3D Hybrid Network of I^1O^2 Topology

Robert Podgajny, Szymon Chorąży, Wojciech Nitek, Michał Rams, Maria Balanda and Barbara Sieklucka

Supporting Information

1. Synthetic strategy

Figure S1. Synthetic strategy: possible bridging between $\{Mn^{II}_9W^{V}_6\}$ clusters occurring *via* the substitution of labile solvent molecules at $[Mn^{II}(NC)_3(MeOH)_3]^-$ units by: organic N-donor linker (a) or/and CN^- (b).

2. Experimental details

Table S1. Changes in the composition of **1** during drying on the air.

3. Crystal structure solution and refinement details

Table S2. Crystal data and structure refinement for **1**.

Table S3. Detailed structure parameters for **1.**

4. Crystal structure visualization

Figure S2. Detailed labeling schemes for **1**: first coordination spheres of Mn5, Mn6, Mn8 and W3 centers (a), first coordination spheres of Mn4, Mn7, W1 and W2 centers (b) and relative positions of metal ions in **1** (c).

Figure S3. Intercluster contacts between $\{Mn_9W_6\}$ units.

5. Magnetic properties

Figure S4. *ac* $\chi'(T)$ (a) and $\chi''(T)$ (b) susceptibility curves for sample **1a** measured at H_{ac}=3 Oe, f = 10 Hz.

1. Synthetic strategy

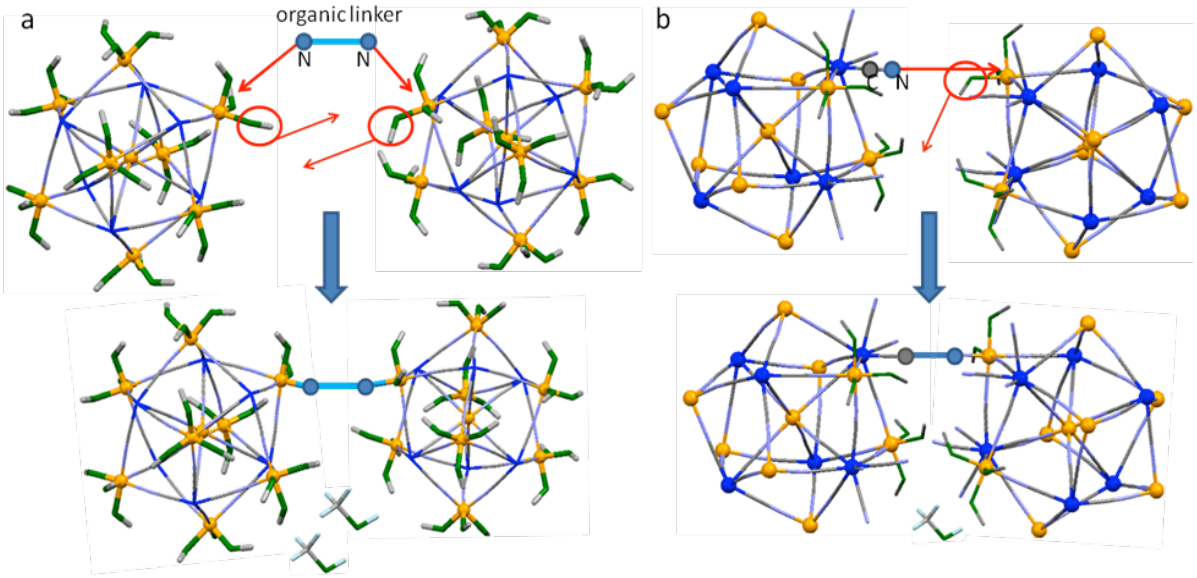

Figure S1. Synthetic strategy: possible bridging between $\{Mn^{II}_9W^{V}_6\}$ clusters occurring *via* the substitution of labile solvent molecules at $[Mn^{II}(NC)_3(MeOH)_3]^-$ units by: organic N-donor linker (a) or/and CN^- (b). Colors: Mn(II) centers (yellow), W(V) centers (dark blue), oxygen atoms of MeOH (green), carbon atoms (grey), nitrogen atoms (pale blue). Some terminal ligands are omitted for clarity. Atom spheres of intercluster bridges are enlarged. Red arrows show changes in coordination spheres during bridging.

2. Experimental details

Materials

$Mn^{II}(ClO_4)_2 \cdot 6H_2O$, 1,2-di(4-pyridyl)ethylene (dpe) and solvents used during the synthesis were purchased from commercial sources (Sigma Aldrich, Idalia) and used without further purification. $Na_3[W(CN)_8] \cdot 4H_2O$ was synthesized according to the published procedure.[S1]

(S1) Samotus, A. *Pol. J. Chem.* **1973**, *47*, 653).

Synthesis, composition and general properties of $\{Mn^{II}_9[W^{V}(CN)_8]_6(dpe)_5(MeOH)_{10}\} \cdot 14MeOH$, 1

Different combinations of organic solvents including alcohols, acetone, acetonitrile, tetrahydrofurane, DMF and DMSO including also some amount of formic acid or acetic acid were used to conduct the self-assembly between $\{Mn_9W_6\}$ clusters and dpe. The best quality crystals of **1** were obtained as follows. 45 mL of methanol, 45 mL of ethanol and 10 mL of acetonitrile were stirred together for several minutes to give solution **I**. A 0.15 mmol (80,4 mg) of $Na_3[W(CN)_8] \cdot 4H_2O$ with 0.225 mmol (81.4 mg) of $Mn^{II}(ClO_4)_2 \cdot 6H_2O$ were dissolved in 6 mL of solution **I** to give light brown solution **II**. A 1,125 mmol (205 mg) of dpe was dissolved in 6mL of solution **I** to give solution **III**. Solution **I** (*ca.* 1 mL) was put into one arm

and solution **II** (*ca*. 1 mL) was put into the other arm of 10 mL H-tube. Then the two arms were filled with solution **I**. After slow diffusion for about five weeks, orange blade crystals of **1** were formed. Both, washing crystals with solution **I** and removal the solvents lead to the breakdown of the crystals after few minutes. Resultant freshly dried powder $Mn_6W_9(dpe)_5(MeOH)_{18}(H_2O)_6$ **1a** was characterized by elementary analysis (Table S1) and IR spectroscopy. IR (KBr pellets) in cm^{-1}: 2170m, 2130m(sh), ν(C≡N); 1552w, 1504w, 1465vw, 1425m, 1350vw cm^{-1}, ν(C=C) and ν(C=N); 1249w, 1220w, 1203w, 1067w, 975w, 960w, 828m, 800m, γ(C-H) and aromatic ring deformations; 1610s, δ(H_2O); 1015m(sh), ν(C-O) (in MeOH); 552m, 465m, coordination. After 24 hours of exposition to the air $Mn_6W_9(dpe)_5(H_2O)_{24}$ **1b** residue was obtained with water as only solvent in the structure. The process of exchange of MeOH to H_2O molecules was confirmed by IR spectra, where the increase of intensity of the bands related to water (especially 1610 cm^{-1}) and the vanishing of 1015 cm^{-1} band related to methanol were observed. Two distinguishable bands 2170m, 2130m(sh) cm^{-1} confirm the presence of bridging W^V-CN-Mn and terminal W^V-CN coordination arrangements.[S2] The region characteristic for vibrations of organic molecules exhibits the set of bands assignable to the vibrations of dpe ligand. The composition of **1** was determined based on the X-ray diffraction measurements. The number of MeOH molecules in **1** and the effective molar mass has been estimated from the elemental analyses of **1a** and **1b**, assuming the total number of solvent molecules to be 24.

Table S1. Changes in the composition of **1** during drying on the air.

Sample	Composition established by	Experimental			General formula: $\{Mn^{II}_9(dpe)_5\,[W^V(CN)_8]_6\}\cdot xMeOH\cdot yH_2O$		Calculated			Molar mass [g/mol]
		C[%]	H[%]	N[%]	x	y	C[%]	H[%]	N[%]	
1	X-ray diffraction, trend of the elemental analyses of 1a and 1b	-	-	-	**24**	**0**	35.0	3.2	17.9	4526
1a	elemental analysis	34.2	2.8	18.7	**18**	**6**	34.1	3.0	18.3	4442
1b	elemental analysis	30.9	2.1	18.9	**0**	**24**	31.0	2.4	19.4	4190

(S2) Podgajny, R. at al, *Dalton Trans*. **2003**, 3458-3468

Physical techniques

Elemental analyses (C, H, N) were performed using an EuroEA EuroVector elemental analyzer. Infrared spectra were measured in KBr pellets between 4000 and 400 cm^{-1} using a Bruker EQUINOX 55 FT-IR spectrometer. Magnetic measurements were performed using Quantum Design SQUID magnetometer MPMS-XL. The sample of **1** was washed from the mother liquor, immersed in solution **I** and closed in a glass tube. Diamagnetic signal of components of solid **1** as well as 120mg of solution I was subtracted. The mass of **1** was estimated to be 23,5(0,5) mg. It was also confirmed by the value of magnetic signal measured at 298 K for sample **1a**. *AC* susceptibility measurements was made at H_{ac} = 3 Oe, at frequencies 1-1000 Hz, down to 1.8 K.

3. Crystal structure solution and refinement

Due to low stability of crystals of **1** many preliminary X-ray diffraction measurements have been done. Three independent full data collection for the determination of the crystal structure of **1** has been performed. To prevent the escape of the solvent molecules from the crystal lattice, in two experiments single crystals were placed in a capillary in vapour of the mother liquor. In the third case a crystal was quickly removed from the mother solution and cooled to 100 K. In each case quality of collected data was weak. The resolution of the data was low, and the values of R_1 and wR_2 factors for the structure refinement were high. In all three cases the crystal structure models obtained from the solution of phase-problem were very similar. This suggests that the data and the model obtained can be considered as reliable. Finally, the data collected at low temperature were chosen for further calculation, as they were the most promising to give the correct model of crystal structure after refinement.
Diffraction data for single crystal were collected on a Nonius KappaCCD four circle diffractometer, equipped with a Mo (0.71073 Å) Kα radiation source, graphite monochromator and CryoStream system for measurements at low temperature. Cell refinement and data reduction was performed using HKL SCALEPAC and DENZO.[S3] Positions of most of non-hydrogen atoms were determined by direct methods using SIR-97.[S4] Non-hydrogen atoms missing in structure model were found on the difference electron density map during structure refinement. Tungsten and manganese atoms were refined anisotropically using weighted full-matrix least-squares on F^2. Other non-hydrogen atoms were refined with isotropic displacement parameters. Attempts to refine these atoms anisotropically makes the refinement process unstable. All hydrogen atoms were positioned with an idealized geometry and refined using a riding model. Refinement and further calculations were carried out using SHELXL-97.[S5] To maintain the correct geometry, selected cyanide groups and selected fragments of ligand molecules of dpe, *trans*-1,2-di(4-pyridyl)ethylene), were refined with restrained distances and angles. In one case, the aromatic ring of the dpe were refined as disordered, in two equally occupied positions. It should be noted that large cavities are present in the obtained model of the crystal structure of **1**. It seems obvious that this cavities are filled with molecules of mother liquor, but, determination of their positions is impossible with the diffraction data obtained.

(S3) Otwinowski, Z.; Minor, W. **1997**. *Methods in Enzymology*, Vol. 276, *Macromolecular Crystallography*, Part A, edited by C. W. Carter Jr & R. M. Sweet, pp. 307-326. New York: Academic Press.

(S4) Altomare, A.; Burla, M. C.; Camalli, M.; Cascarano; G. L., Giacovazzo, C.; Guagliardi, A.; Moliterni, A. G. G.; Polidori, G.; Spagna, R. *J.*, *Appl. Cryst.* **1999**, *32*, 115-119.

(S5) Sheldrick, G. M., *Acta Cryst.* **2008**, *A64*, 112-122.

(S6) Farrugia, L. J., *J. Appl. Cryst.* **1997**, *30*, 565.

(S7) Farrugia, L. J., *J. Appl. Cryst.* **1999**, *32*, 837-838.

The checkcif comments

The checkcif alerts:

```
THETM01_ALERT_3_A
PLAT201_ALERT_2_A
PLAT220_ALERT_2_A
PLAT220_ALERT_2_A
PLAT602_ALERT_2_A
DIFMX01_ALERT_2_B
PLAT094_ALERT_2_B
PLAT097_ALERT_2_B
PLAT342_ALERT_3_B
PLAT731_ALERT_1_B
DIFMX02_ALERT_1_C
RFACG01_ALERT_3_C
RFACR01_ALERT_3_C
PLAT029_ALERT_3_C
PLAT082_ALERT_2_C
PLAT084_ALERT_2_C
```

are a direct consequence of relatively weak quality of diffraction data and high degree of disorder, particularly in the space of crystallization solvent molecules.

The checkcif alerts PLAT241_ALERT_2 and PLAT242_ALERT_2 on levels A and B are typical for complexes with central metal ion and mobile organic ligands.

Table S2 Crystal data and structure refinement for **1**

Empirical formula	$Mn_9W_6C_{108}H_{50}N_{58}O_{10}$
Formula weight	3917.62
Temperature	100(2) K
Wavelength	0.71069 Å
Crystal system	Monoclinic
Space group	C2/c
Unit cell dimensions	a = 41.686(5) Å
	b = 19.050(5) Å
	c = 29.292(5) Å
	α = 90.000(5)°
	β = 120.028(5)°
	γ = 90.000(5)°
Volume	20139(7) $Å^3$
Z	4
Density (calculated)	1.292 Mg/m^3
Absorption coefficient	4.002 mm^{-1}
F(000)	7412
Crystal size	0.32 x 0.15 x 0.03 mm^3
Theta range for data collection	1.13 to 21.00°
Index ranges	$-40 \leq h \leq 41$, $-15 \leq k \leq 19$, $-29 \leq l \leq 29$
Reflections collected	26188
Independent reflections	10488 [R(int) = 0.0612]
Completeness to theta = 21.00°	97.0 %
Absorption correction	Semi-empirical from equivalents
Max. and min. transmission	0.8894 and 0.3607
Refinement method	Full-matrix least-squares on F^2
Data / restraints / parameters	10488 / 65 / 439
Goodness-of-fit on F^2	1.120
Final R indices [I>2sigma(I)]	R1 = 0.1283, wR2 = 0.3172
R indices (all data)	R1 = 0.1456, wR2 = 0.3339
Largest diff. peak and hole	11.508 and -2.216 $e.Å^{-3}$

Table S3 Detailed structure parameters for **1**

Metal center			Metal center		
W1	W-C	2.09-2.20Å	Mn6	Mn-N23	2.20(2)Å
	C-N	1.12-1.21Å		Mn-N16	2.17(3)Å
	W-C-N	174-178°		Mn-N26	2.23(3)Å
				Mn-N36	2.18(2)Å
W2	W-C	2.11-2.18Å		Mn-N621	2.27(2)Å
	C-N	1.12-1.24Å		Mn-N611	2.27(2)Å
	W-C-N	171-178°		Mn-N23-C23	165(2)°
				Mn-N16-C16	177(2)°
W3	W-C	2.14-2.19Å		Mn-N26-C26	171(2)°
	C-N	1.10-1.34Å		Mn-N36-C36	169(2)°
	W-C-N	171-178°		N23-Mn-N16	90.7(9)°
				N23-Mn-N26	100.4(9)°
Mn4	Mn-N14	2.21(3)Å		N23-Mn-N36	86.7(9)°
	Mn-N24	2.19(3)Å		N23-Mn-N611	89.2(9)°
	Mn-N34	2.23(2)Å		N23-Mn-N611	87.0(9)°
	Mn-N14-C14	169(3)°		N16-Mn-N26	92.4(9)°
	Mn-N24-C24	168(3)°		N16-Mn-N36	88.4(9)°
	Mn-N34-C34	166(2)°		N16-Mn-N611	179.5(12)°
	N14-Mn-N14	180.0(5)°		N16-Mn-N621	89.6(9)°
	N24-Mn-N24	180.0(9)°		N26-Mn-N36	86.7(9)°
	N34-Mn-N34	180.0(14)°		N26-Mn-N611	88.2(10)°
	N14-Mn-N24	86.1(10)° 93.9(10) °		N26-Mn-N621	172.4(9)°
	N24-Mn-N34	88.9(9)° 91,9(9) °		N36-Mn-N611	91.7(9)°
	N34-Mn-N14	89.6(9)°		N36-Mn-N621	86.0(9)°
				N621-Mn-N611	89.9(10)°

		90.4(9) °			
Mn5	Mn-N11	2.21(2)Å	Mn7	Mn-N17	2.18(3)Å
	Mn-N15	2.23(3)Å		Mn-N27	2.19(3)Å
	Mn-N25	2.21(3)Å		Mn-N37	2.21(3)Å
	Mn-N35	2.263(15)Å		Mn-N711	2.25(2)Å
	Mn-N511	2.29(3)Å		Mn-O71	2.18(3)Å
	Mn-N521	2.29(2)Å		Mn-O72	2.14(3)Å
	Mn-N11-C11	167(2)°		Mn-N17-C17	174(3)°
	Mn-N15-C15	176(2)°		Mn-N27-C27	170(2)°
	Mn-N25-C25	172(3)°		Mn-N37-C37	164(3)°
	Mn-N35-C35	145(3)°		N17-Mn-N27	94.4(10)°
	N11-Mn-N15	103.7(9)°		N17-Mn-N37	91.3(11)°
	N11-Mn-N25	87.8(9)°		N17-Mn-N711	87.4(10)°
	N11-Mn-N35	166.9(11)°		N17-Mn-O71	86.0(11)°
	N11-Mn-N521	88.6(8)°		N17-Mn-O72	176.9(12)°
	N11-Mn-N511	85.7(9)°		N27-Mn-N37	94.0(11)°
	N15-Mn-N25	94.1(10)°		N27-Mn-N711	88.1(10)°
	N15-Mn-N35	85,4(11)°		N27-Mn-O71	175.2(11)°
	N15-Mn-N521	87.0(9)°		N27-Mn-O72	88.7(11)°
	N15-Mn-N511	168.4(10)°		N37-Mn-N711	177.6(11)°
	N25-Mn-N35	82.1(11)°		N37-Mn-O71	90.8(11)°
	N25-Mn-N521	176.4(9)°		N37-Mn-O72	88.2(12)°
	N25-Mn-N511	92.9(10)°		N711-Mn-O71	87.2(11)°

	N35-Mn-N521	101.4(11)°		N711-Mn-O72	92.9(11)°
	N35-Mn-N511	86.5(12)°		O71-Mn-O72	91.0(12)°
	N521-Mn-N511	86.5(10)°			
Mn8	Mn-N18	2.22(3)Å	Mn8	N18-Mn-N28	90.5(10)°
	Mn-N28	2.16(3)Å		N18-Mn-N38	97.4(10)°
	Mn-N38	2.21(3)Å		N18-Mn-O82	89.9(11)°
Mn8	Mn-O82	2.18(3)Å	Mn8	N18-Mn-O83	176.5(12)°
	Mn-O83	2.24(4)Å		N18-Mn-O84	93.7(13)°
	Mn-O84	2.23(4)Å		N28-Mn-N38	95.6(11)°
	Mn-N18-C18	163(2)°		N28-Mn-O82	174.5(12)°
	Mn-N28-C28	171(3)°		N28-Mn-O83	90.2(12)°
	Mn-N38-C38	174(3)°		N28-Mn-O84	90.4(13)°
				N38-Mn-O82	89.8(11)°
				N38-Mn-O83	85.9(12)°
				N38-Mn-O84	167.2(13)°
				O82-Mn-O83	89.1(13)°
				O82-Mn-O84	84.1(14)°
				O83-Mn-O84	82.8(14)°

4. Crystal structure visualization

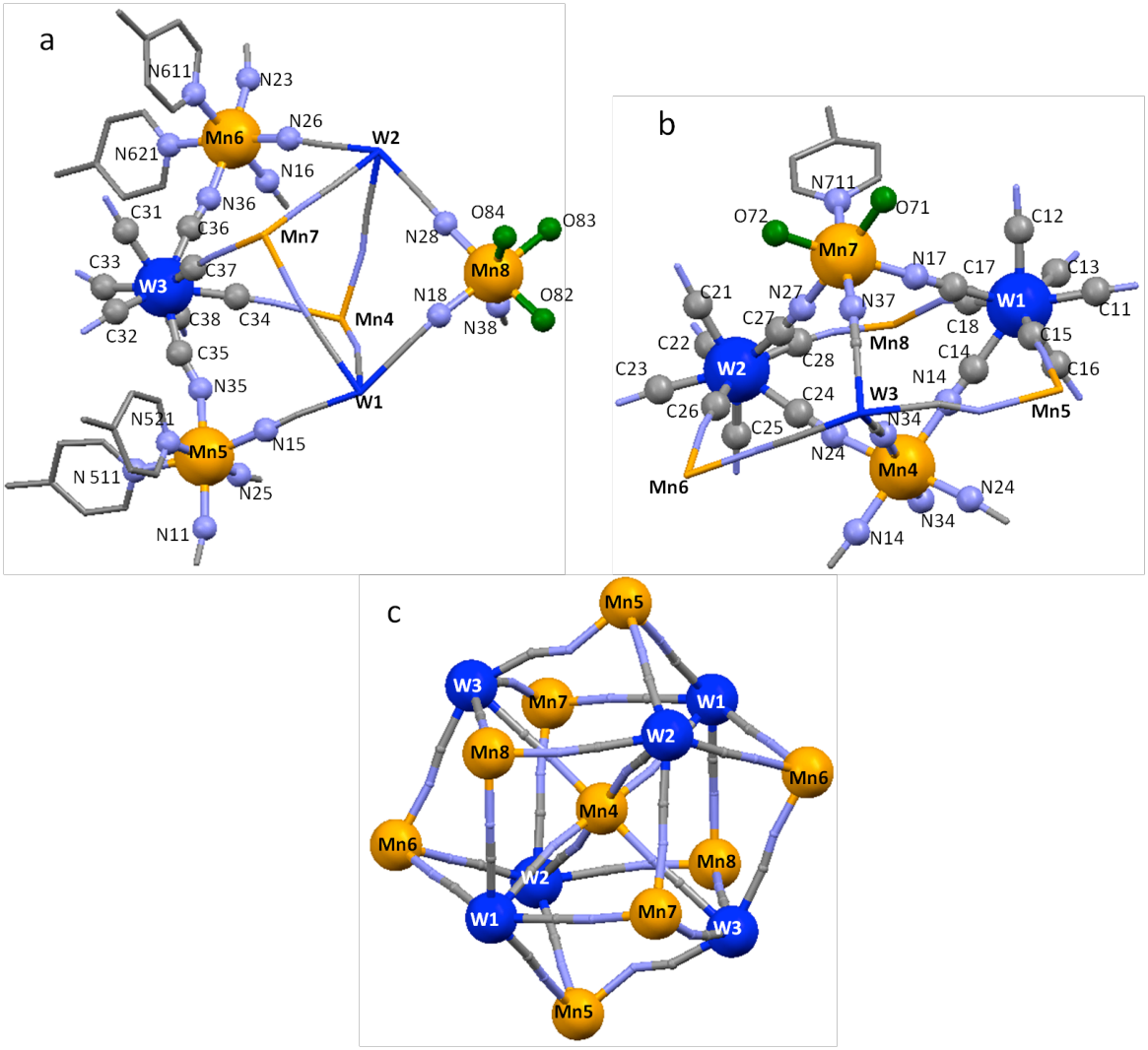

Figure S2. Detailed labeling schemes for **1**: first coordination spheres of Mn5, Mn6, Mn8 and W3 centers (a), first coordination spheres of Mn4, Mn7, W1 and W2 centers (b) and relative positions of metal ions in **1** (c). Colours: Mn(II) centers (yellow), W(V) centers (dark blue), oxygen atoms of MeOH (green), carbon atoms (grey), nitrogen atoms (blue). Hydrogen atoms and terminal ligands (in c) are omitted for clarity. Atom spheres of metal centers and atoms from first coordination sphere of metals (in a and b) are enlarged.

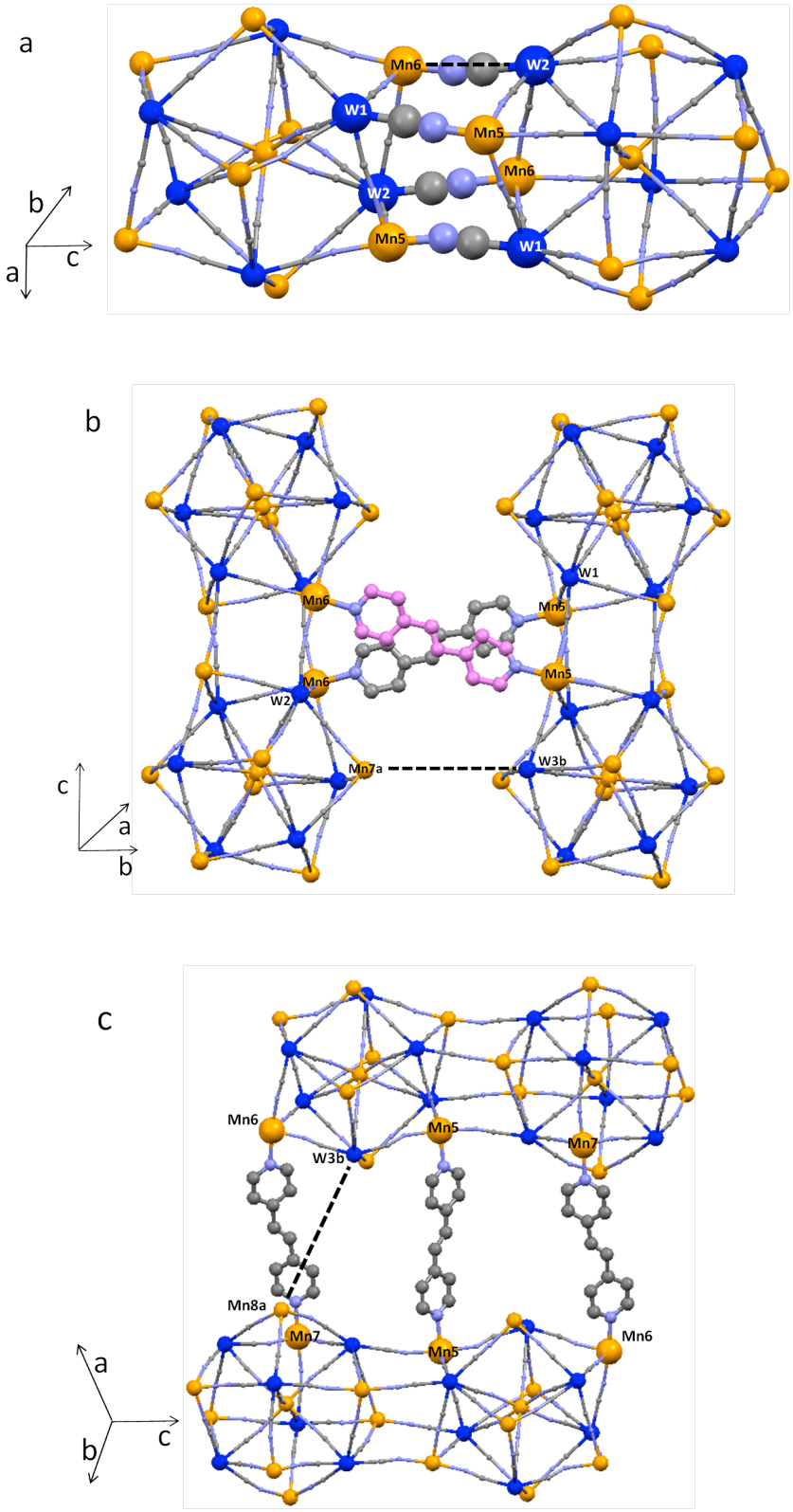

Figure S3. Intercluster contacts between $\{Mn_9W_6\}$ units. Dotted line illustrate the closest intermolecular contacts in the directions orthogonal to the direction *c* of $\{Mn_9W_6\}_4$ nanowire.

5. Magnetic properties of 1a

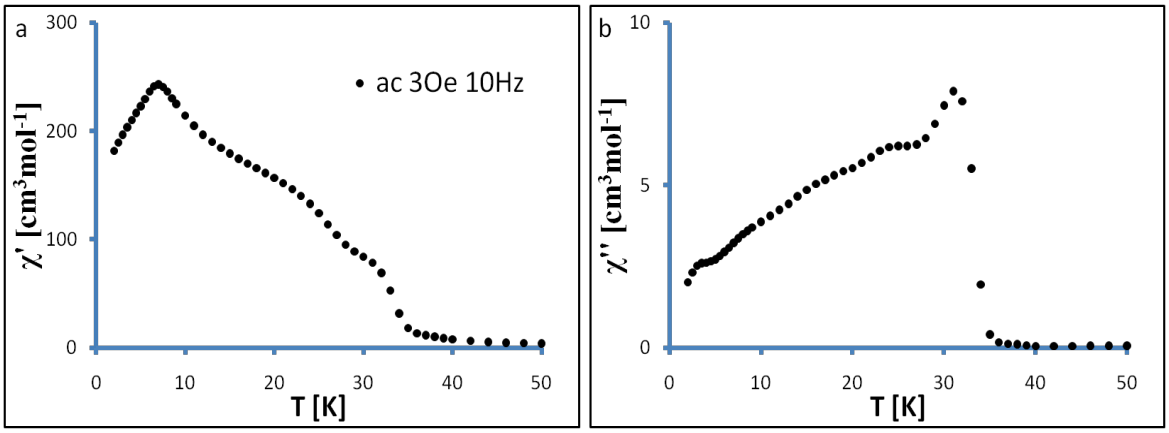

Figure S4. *ac* $\chi'(T)$ (a) and $\chi''(T)$ (b) susceptibility curves for sample **1a** measured at H_{ac}=3 Oe, f = 10 Hz.